Figures of merit for laser beam quality

T.D. Milster and E.P. Walker
Optical Sciences Center
University of Arizona, Tucson, Arizona 85721

ABSTRACT

We show how FWHM, FW1/e², Strehl ratio, and encircled energy figures of merit vary with different types of aberration and measurement methods. We examine in detail the array sampling method and the slit-scan method. Our irradiance in the exit pupil of the optical system is a simple gaussian. We found that in general the slit-scan method and the array method do not yield the same result. The width measurements for the central lobe of the diffraction pattern are very insensitive to aberration.

2. INTRODUCTION

As has been known since opticists started making lenses, aberrations redistribute energy from the central lobe of the Airy pattern into the sidelobes. However, the study of the effects of aberrations in laser beam systems with nonuniform irradiance profiles is a relatively new topic [1][2][3]. For example, a full-width at half maximum (FWHM) of the central lobe in a focused beam that is near the value obtained with an unaberrated system is often used as justification that the beam is "diffraction limited." In this paper, we show that caution must be used in drawing this conclusion because of the effects third-order aberrations have on the FWHM. We also describe how several figures of merit vary with aberrations and measurement technique.

Two methods used to measure laser beam quality are sampling an array of data points and measuring with a scanning slit [3]. We can obtain a two-dimensional array of sample points by inserting a CCD camera or a scanning pinhole directly into the beam. Line profile and edge response data are obtained by scanning a slit across the beam. Instruments used to obtain array and scanning slit data are typically much simpler and less expensive than interferometers, which is a third alternative to measure beam quality. In this paper, we concentrate on the properties of array and slit-scan measurements of a focused laser beam.

Common figures of merit for laser beam quality include width measurements, Strehl ratio, and encircled energy, as shown in Figure 1. FWHM and full-width at $1/e^2$ (FW1/e²) are self explanatory. The Strehl ratio is defined as the ratio of the peak irradiance of the aberrated beam, I*, to the peak irradiance, I, of a system with no aberrations. Encircled energy is defined as the ratio of the power, P*, contained in a small circular region around the peak of the aberrated beam to the total power, P, in the beam. Our circular region is equal to the diameter of the first ring of the Airy pattern in an aberration-free and uniformly illuminated system. This diameter is 1.22 λ/NA, where λ is the laser wavelength and NA is the numerical aperture of the focused beam. A related figure of merit is the energy ratio of the power outside the circular area to
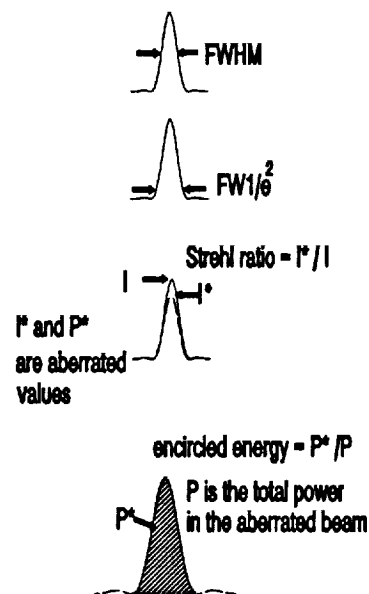

Figure 1. Figures of merit.

the total power in the beam, which can be calculated from: energy ratio $= 1 - P'/P$.

Our optical system model is shown in Figure 2. A simple gaussian laser beam is reimaged through an optical system so that the waist is located a distance R from the exit pupil. The laser beam irradiance in the exit pupil has a FW1/e^2 of 2w. The stop has diameter d. We assume that d $>>$ λ and that the NA is large enough so that focus shifts due to the properties of the gaussian beam are insignificant. We also assume that the NA is small enough so that vector diffraction effects are not significant. We model the effects of aberrations by adding a phase error, ΔW, to the wavefront in the exit pupil. The phase errors take the form of astigmatism (W_{222}), spherical (W_{040}) and coma (W_{131}).
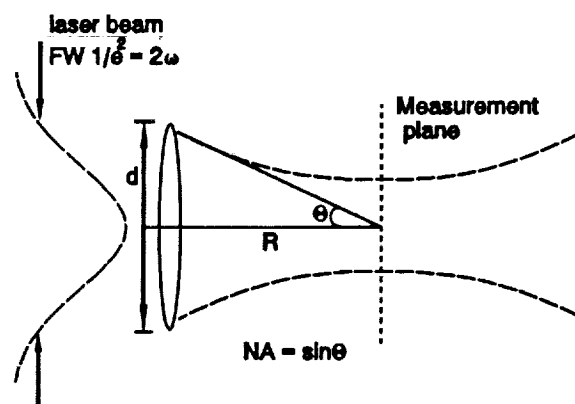
Figure 2.   Optical system model.

In the following paragraphs we review array and slit-scan methods. Then we discuss effects of individual third-order aberrations on various figures of merit. Next we discuss effects of random combinations of third-order aberrations. We then summarize and present our conclusions.

3. REVIEW OF ARRAY AND SLIT-SCAN METHODS

Array methods include scanning a pinhole over the measurement plane or using a two-dimensional array of detectors, like those found in a charge-coupled device (CCD) camera. In either case, a two-dimensional data set is acquired from which the figures of merit are calculated. The data are discrete samples of the irradiance incident onto the measurement plane. In order to provide sufficient sampling, the spacing between detector elements must be small compared to the beam size. Typically, CCD cameras have pixel sizes on the order of 10 μm on a side. This limits the practical beam sizes that can be measured to several hundred microns. An auxiliary lens may be used to produce a magnified image of a

Figure 3.   (a) slit-scan method. (b) edge scan method.

smaller beam onto the detector plane, but additional aberrations are often introduced that affect the measurement. Also, care must be taken in interpreting metric information from the array, because pixels in CCD cameras are often not square nor do they have the same interval in the horizontal and vertical directions. In our study we assume that the pixels are square and uniformly spaced.

Slit-scan methods are used to derive one-dimensional information from the laser beam. As shown in Figure 3A, a narrow slit is used to scan the measurement plane in the x direction. The slit integrates the irradiance in the y direction, so data do not represent true beam profiles, but rather they represent projections along the y axis. The width of the slit determines the resolution of the measurement. Ideally, an infinitely narrow slit would be used, but as the slit becomes too narrow the signal-to-noise degrades.
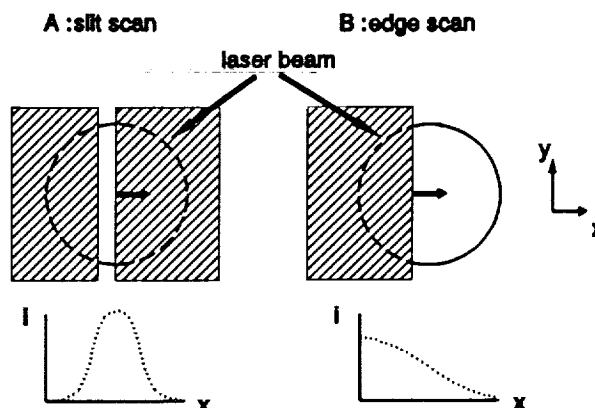
Another way to obtain slit-scan data is from a moving knife edge, as shown in Figure 3B. In this case, an opaque surface with a sharp edge is scanned across the measurement plane in the x direction. The data from the edge scan are differentiated, and the result is equivalent to an infinitely narrow slit scan, except that the signal-to-noise is improved because more signal light is available.

4. EFFECTS OF INDIVIDUAL THIRD-ORDER ABERRATIONS

In this section we examine the effects of astigmatism, spherical aberration and coma on several figures of merit. Both array data and slit-scan methods are implemented. In our study, we use a simple scalar diffraction modeling code. The optical system is such that $2w/d = 0.89$, which corresponds to the optimum overfill in terms of maximum peak irradiance in the focused beam [4]. In a real optical system, defocus and tilt can be adjusted to give a higher beam quality by canceling some of the effects of aberrations. In our modeling we add the appropriate amount of defocus and tilt to minimize the root-mean-square (rms) wavefront error. The amount of phase error, ΔW, added to the ideal wavefront for each aberration is described by the peak error at the edge of the exit pupil before correction. Width measurements are normalized with respect to NA and λ. For a specific optical system, the physical width is found by multiplying the normalized value by λ/NA.

Figure 4. Normalized FWHM and FW $1/e^2$ of the array and slit-scan methods as a function of astigmatism.

We consider the FWHM figure of merit first. Figure 4 displays the normalized FWHM versus astigmatism for the array and slit-scan methods. The laser beam exhibits a symmetric profile in the measurement plane because defocus has been added to minimize the rms wavefront error. There is little change in the FWHM measurement for less than one wave of astigmatism. The array method and the slit-scan method produce similar results. Figure 5 displays the normalized FWHM versus spherical aberration. Sidelobes due to more than two waves of spherical aberration affect width measurements significantly. Lobe widths plotted in Figure 5 include the maximum FWHM (that including all of the sidelobes), central-lobe FWHM and side-lobe FWHM. As the amount of aberration increases, the FWHM of the central lobe actually decreases for the array method. The slit-scan method is slightly more sensitive. The jump in the FWHM around 2.4 waves is due to the shape of the sidelobes in the slit-scan method. As shown in Figure 6A, the slit scan of a beam having 2.4 waves of spherical aberration has sidelobes that increase
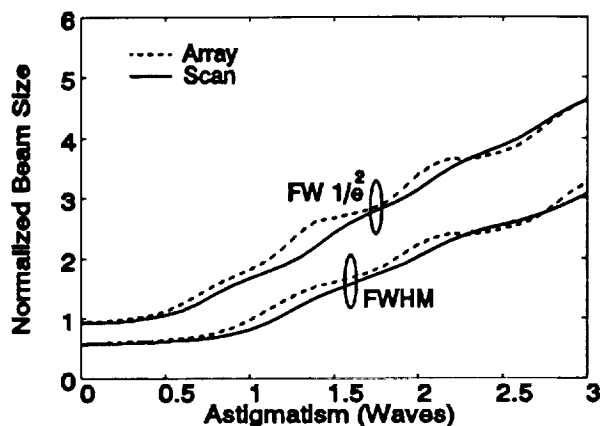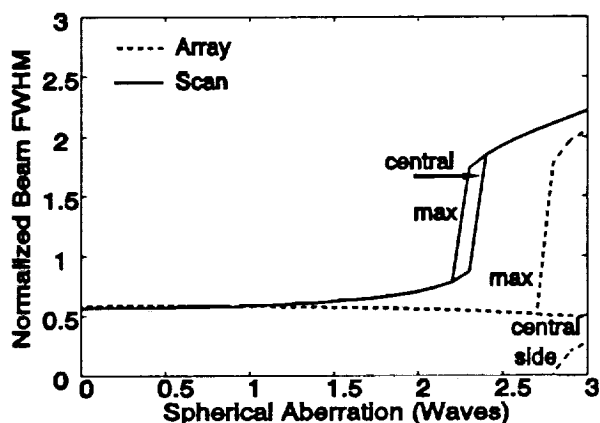

Figure 5. Normalized FWHM of the array and slit-scan methods as a function of spherical aberration.

the FWHM. With 2.3 waves of spherical aberration, the sidelobes are below the half-maximum of the irradiance peak. In Figure 6B, we show the array profile of the beam with 2.4 waves of spherical aberration. Note that the central lobe is well defined, and the sidelobes are well below the half-maximum of the peak irradiance. Figure 7 displays the normalized FWHM versus coma. Coma is not a symmetric aberration, so we consider profiles and slit-scans in both the x and y directions. Again, FWHM is insensitive below one wave of aberration. Sidelobes affect the FWHM measurement at about 2.6 waves of coma. An oscillatory property is observed for the FWHM of the central peak in the x direction, which is also the direction of the maximum wavefront error in the uncorrected system.
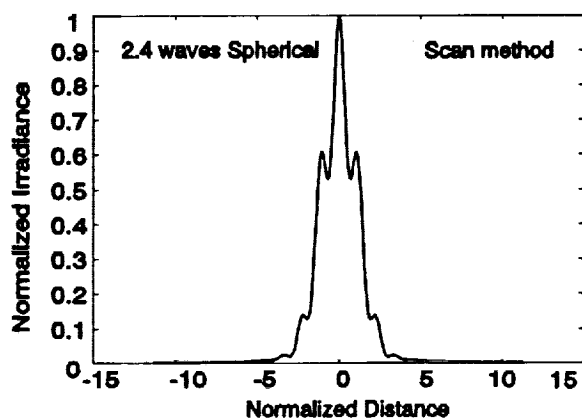

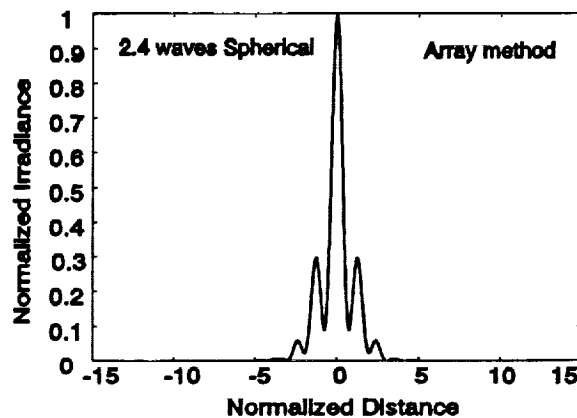Figure 6a.   Irradiance profile of the slit-scan method with 2.4 waves of spherical aberration.

Figure 6b.   Irradiance profile of the array method with 2.4 waves of spherical aberration.

Next we consider $FW1/e^2$. Figure 4 displays the $FW1/e^2$ for astigmatism. A monotonically increasing curve is observed for the slit-scan method, and the array method is more oscillatory, but it is well behaved. Figure 8 displays $FW1/e^2$ for spherical aberration. As was observed for FWHM, the sidelobes affect the $FW1/e^2$ figure of merit dramatically. Note that, for the central lobe in the array method, the $FW1/e^2$ actually decreases with increased spherical aberration. Sidelobes increase the maximum $FW1/e^2$ at 1.9 waves for the array method and at 1.2 waves for the slit-scan method. Figure 9 displays $FW1/e^2$ versus coma. Due to the asymmetric behavior of the focused beam the $FW1/e^2$ figure of merit becomes complicated to

Figure 7.   Normalized FWHM of the array and the slit-scan methods as a function of coma.

interpret above one wave of coma. In general, the slit-scan method is more sensitive. Note that for all three aberrations the $FW1/e^2$ figure of merit is not sensitive below 0.5 wave of aberration.

We now discuss Strehl ratio. Figure 10 displays the Strehl ratio for all three aberrations and both measurement methods. For the array method , Strehl ratio is a very sensitive figure of merit. For the slit-scan method, Strehl ratio is not as sensitive, but it does provide a monotonically decreasing figure of merit with increased aberration. Both methods, Strehl ratio is most sensitive to
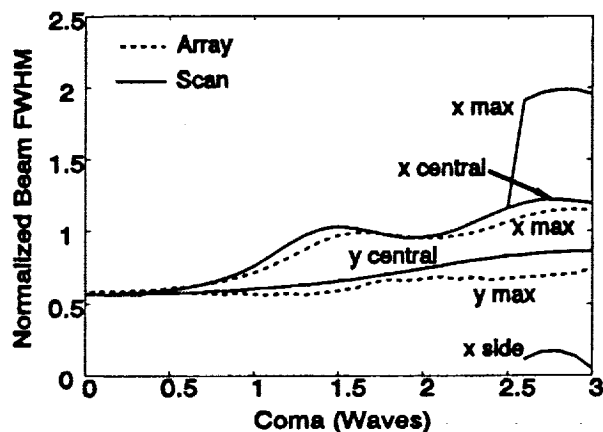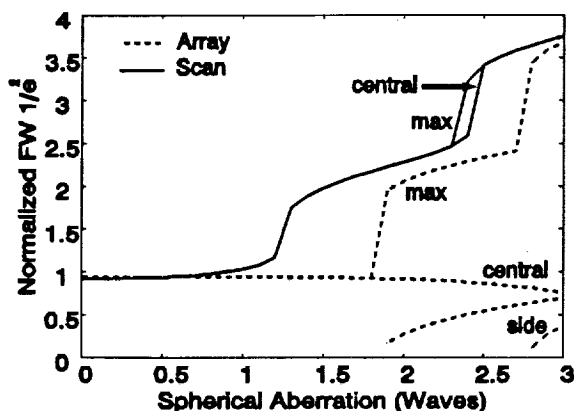
156

astigmatism.

Figure 8. Normalized FW $1/e^2$ of the array and slit-scan methods as a function of spherical aberration.
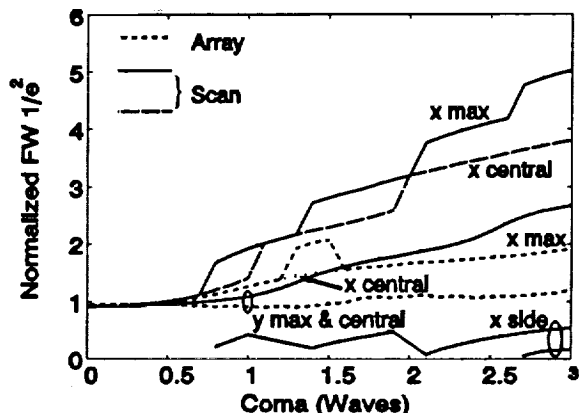

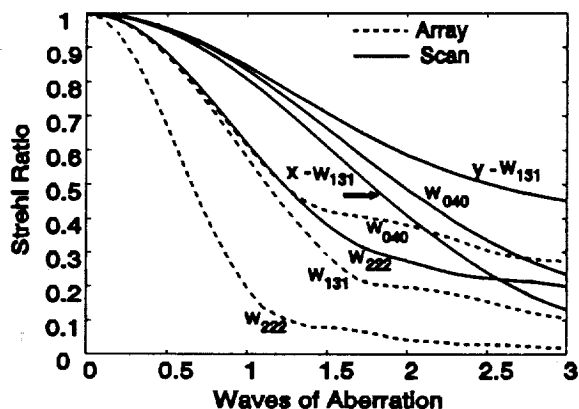Figure 9. Normalized FW $1/e^2$ of the array and the slit-scan method as a function of coma.

Figure 10. Strehl ratios of the array and slit-scan methods as a function of waves of aberration.
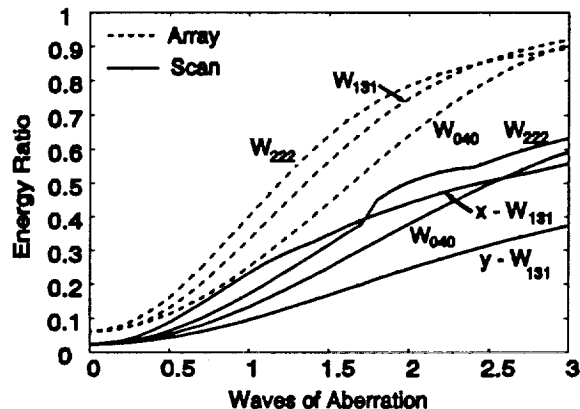

Figure 11. Energy ratio of the power outside of the central lobe to the total power in the beam.

Figure 11 displays the energy ratio for all three aberrations and both measurement methods. Like we observed in the Strehl ratio calculations, the energy ratio is a smooth monotonic function versus aberration. The array method is more sensitive than the slit-scan method. Coma and astigmatism are more easily detected than spherical aberration. When data in Figure 11 is compared to the width data in Figures 4, 5, and 7-9, we observe that the insensitivity of the FWHM can be a severe problem. For example, up to 40% of the total spot energy is contained outside the central lobe for one wave of aberration. Although FW$1/e^2$ is slightly more sensitive, up to 18% of the total spot energy is contained outside of the central lobe for one-half wave of aberration.

5. EFFECTS OF COMBINED ABERRATIONS

We study the effects of combined aberrations with a simple extension to our basic model. Instead of a single aberration, we included random amounts of astigmatism, spherical, and coma. In addition,

the coma rotation angle and the astigmatism rotation angle were included as random variables. Tilt and defocus were added in order to minimize the rms wavefront departure. Standard deviation of the wavefront, σ, was kept between the limits : $0 \leq \sigma \leq 0.10$. The overfill of the laser beam in the exit pupil was slightly different in the x and y directions. A total of 2000 trials were performed. The figures of merit for both the array method and the slit-scan method were calculated for each trial. The result of the average FWHM versus σ is shown in Figure 12, which displays similar characteristics to Figures 5 and 7 for low values of aberration. The difference between the focused beam width in the x and y directions is due to the difference in overfill in the exit pupil. The slit-scan method

Figure 12. Normalized FWHM of the array and slit-scan methods as a function of wavefront standard deviation.

produces smaller beam widths than the array method for $\sigma < 0.07$ and larger beam widths for $\sigma > 0.08$. The relation between σ and the peak ΔW depends on the type of aberration present. For example, one wave of astigmatism has $\sigma = 0.200$, one wave of spherical has $\sigma = 0.074$, and one wave of coma has $\sigma = 0.116$.
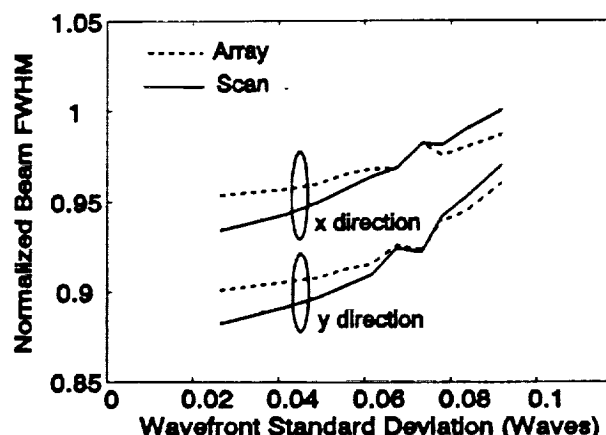
6. SUMMARY AND CONCLUSIONS

We have shown how FWHM, FW1/e^2, Strehl ratio, and encircled energy figures of merit vary with different types of aberration and measurement methods. We found that in general the slit-scan method and the array method do not yield the same result because the slit-scan method measures an integrated line profile of the beam while the array method measures a profile. The FWHM and FW1/e^2 values for the central lobe of the diffraction pattern are very insensitive to aberration. Therefore, one should use caution when claiming that an optical system is "diffraction limited" based solely on the these criteria. In the case of spherical aberration the central lobe width actually decreases with increased aberration. The slit-scan method width measurements are typically more sensitive to aberration than the array method. The most sensitive figure of merit is the array method Strehl ratio. The array method energy ratio is a useful figure of merit because is it describes the ratio of the power outside the central lobe to the total power in the beam. The numeric values for the energy ratio from a slit-scan are always lower than the corresponding array method. Both the Strehl ratio and the energy ratio are smooth, monotonic functions versus aberration. A computer experiment in which random combinations of aberration are added to the exit pupil indicates that the average FWHM is different for slit-scan and array methods. Our results for individual aberrations are based on one condition of overfill in the exit pupil. Other overfill ratios (2w/d) could yield different results.

7. ACKNOWLEDGEMENTS

8. REFERENCES

1.   A. Siegman, "Effects of spherical aberration on laser beam quality," SPIE 1834, in press.

2.   T.D. Milster, M.K. Benedict, and R.P. Stahl, " Laser diode requirements for magneto-optical storage devices," SPIE 1316, pp. 143-149 (1990).

3.   T.D. Milster and J.P. Treptau, "Measurement of laser spot quality," SPIE 1414, pp. 91-96 (1991).

4.   H.M. Haskill, "Laser recording with truncated gaussian beams," Appl. Opt., vol. 18, no. 3, pp. 2143-2146 (1979).

APPENDIX G

161